EFFECT OF ALKALI TREATED WALNUT SHELL (*JUGLANSREGIA)* ON HIGH PERFORMANCE THERMOSETS. STUDY OF CURING BEHAVIOR, THERMAL AND THERMOMECHANICAL PROPERTIES

A. H. SHAH[a, b], X. LI[a], X. D. XU[a,*], S. WANG[a], J. W. BAI[a], J. WANG[a], W. B. LIU[a]

[a]*Key Laboratory of Superlight Material and Surface Technology, Ministry of Education, College of Materials Science and Chemical Engineering, Harbin Engineering University, Harbin 150001, China*

[b]*Department of Textile Engineering, Balochistan University of Information Technology, Engineering and Management Sciences, Quetta 87300, Pakistan*

This paper presents a comparative analysis of high performance thermosets based on epoxy (Ep) and diaminodiphenylmethane (DDM) and its blend with DDM based benzoxazine (P-ddm); (Ep/P-ddm) with reinforcement using alkali treated walnut shell (TWN) at 10, 20 and 30 wt% reinforcement. Thermogravimetric (TGA) and x-ray diffraction (XRD) analysis of TWN showed improved thermal stability and crystallinity index. On 30 wt% TWN loading, the storage modulus (*G′*) of Ep/DDM system improved by 42%, while the values of *G′* and T_g were enhanced by 58% and 30°C, respectively, on the similar loading in Ep/P-ddm, due to the increased number of functional groups on TWN particles. The degradation temperature peak (DTG) of all composites shifted towards the higher temperatures, which confirms the improved thermal stabilities. The prepared composites can be used in solder drip resistance and fire retardant applications as confirmed from limiting oxygen index and DTG peak value.

(Received May 15, 2018; Accepted September 21, 2018)

Keywords: Biocomposites, Alkali treatment, Walnut shell, Copolymerization, Thermosets

1. Introduction

In recent era, with increased environmental awareness, ecosystems and new legislations, bio wastes are getting primary importance for reinforcement in polymeric matrices [1]. Several researchers have reported the effective utilization of bio wastes in different polymer matrices [2-4]. In this way, both; the polymer matrix gets improved performance characteristics while effective utilization of bio waste is also accomplished. Wastes from agro industry used for making different polymer matrices include almond shell [3, 5], apricot shell [6], wheat straws [7], cotton seed hulls [8], walnut shells [9], wood flour [10] and corn [11]. The compositions of these materials include mostly cellulose, hemicellulose, lignin and other extractives.

Walnut is cultivated worldwide as edible nut. The average production in the years 2010-14 was approximately 3.35 million tons harvested from 1.02 million ha. China was on first place with 1.68 million tons average production [12]. The walnut contains 67% fruit and averagely 0.25 million tons per year of the shell can be generated. The walnut shell has no economical value or industrial usage and the producing countries usually discard or burn it in stoves in the winters. The walnut shell is comparatively different from other biomass as the shell contain lower contents of hygroscopic materials (Cellulose and hemicellulose) and higher amounts of hydrophobic materials (lignin and extracts) [13]. The chemical composition of walnut shell include holocellulose 47.78%, cellulose 26.51%, lignin 49.18%, and ash 2.13% [14].

Particle board from walnut shell using urea–formaldehyde based composite with improved performance is also reported [15]. One researcher also reports densely filled polypropylene composites using walnut shell with improved dimensional stability for outdoor applications [14].

*Corresponding author: xuxiaodong@hrbeu.edu.cn

Composites with low density polyethylene with improved performance is also reported [16]. Fracture toughness and wear response studies conducted on particle board also shows an improved performance of walnut shell particles when embedded in epoxy as a matrix material [17, 18]. Although, a lot of work is already reported for this special class of filler which shows interesting features with improved performance characteristics in resin formulations while no use of this filler is reported for high performance thermosets. High performance thermosets are usually characterized by high mechanical and thermal properties. The glass transition temperature (T_g) of high performance thermosets is considered as an important parameter especially as the network achieves maximum properties after full cure of the network. The performance characteristics of epoxy are dependent on the type of hardener used. An ambient temperature resin/hardener combination does not achieve high performance characteristics resulting in lower thermo mechanical properties like low T_g. In contrast aromatic type hardeners require more heat to form fully cured network and achieves high performance characteristics. The epoxy cured with 4,4-diaminodiphenyl methane (DDM) bear excellent mechanical properties, electrical insulation, high temperature, radiation and wear resistance. Another class of high performance thermosets include diaminodiphenylmethane based benzoxazine (P-ddm), which possess high heat resistance, good dimensional stability, low moisture absorption and no volatiles formation during polymerization, thus offering many advantages for various applications [19, 20]. Literature includes various polybenzoxazine composites made from organic and inorganic fillers [20-23]. It is well reported in literature that incorporation of polybenzoxazines into epoxies improves fire resistance, charring, flexural modulus and strength but reduces the fracture toughness and T_g of the composites [24]. The same research group made an attempt to increase the fracture toughness by rubber toughening. The method was successful for improving fracture energy but T_g values were decreased.

In the view of above discussion, to improve the performance characteristics, the use of filler must contain functional groups for more improvement. Introduction of functional groups in resin molecules improves the performance of resultant composites, which is usually achieved by hydroxyl, phenol and amine containing raw materials [20, 23, 25]. Alkali treatment of natural fillers is also reported to improve the surface characteristics of filler for good filler and resin interactions[26]. After alkali treatment, the filler achieves rough surface along with more groups exposed to the surface for better filler matrix interaction[26].

From composition of walnut shell filler, containing different types of functional groups in the composition we believe that this filler must improve reinforcement effects in high performance thermosets. This paper presents thermal and thermomechanical properties of alkali treated walnut shell particles as a reinforcement in high performance thermosets based on epoxy (Ep) and DDM and blend of Ep and P-ddm composites containing 10, 20, and 30 wt% of walnut shells.

2. Materials and methods

The fresh walnut shells were purchased from the local market and washed with water to remove dirt and dried in oven at 60°C for two days and keep safe for further processing. Diglycidyl ether of bisphenol-A (DGEBA) E-51, a commercial epoxy with a density of 1.26 g/cm^3 and epoxy equivalent weight of 184-195 g/eq. was purchased from Feng Huang Co. Ltd,. China. Diamino diphenyl methane (DDM) having 198.26 g/mol molecular weight, was used as a hardener and purchased from Energy Chemical, China. The P-ddm monomer (99.5%) was kindly donated by Jiangxi Huacui Advanced Materials Co., Ltd, China. Ethanol (99.0%), cyclohexane (99.5%), acetic acid (99.0%), and sodium hydroxide (NaOH) (99.9%) were procured from Shanghai Jingchun Reagent Co. Ltd. China. The deionized water was used throughout the experiments.

2.1 Preparation of particles

The walnut shells (WN) were grinded using grinding mill available in laboratory to reduce the size of the shell. Grinded shells were further reduced in size using high-energy planetary ball mill of Fritsch Pulverisette 7 [27]. Sintered polytetraflouroethylene (PTFE) container with a volume capacity (500 mL) and steel balls of different diameters ranging from 5-25 mm were used

for 72 h of milling with 30 min break after every 1 h to avoid excessive heat generation and degradation of cellulose. The ball to material ratio was kept 15:1 and the speed was set at 450 rpm. The WN flour particles passing through a 200-mesh screen were collected and dried in a laboratory oven at 80°C for 48 h. Alkali treatment of WN was performed by preparing 1% solution of NaOH and the treatment was done for 3 h at liquor ratio of 15:1. After the treatment, the mixture was washed two times with distilled water and ethanol. Finally neutralization of the particles was carried out by a single drop of acetic acid in 50 mL of distilled water and the mixture was kept for 30 min at room temperature. After that the particles were again washed and coded as TWN.

2.2 Preparation of composites

Epoxy E51 (Ep) resin was taken in a glass beaker and put in oil bath already heated at 80°C. This was done to ensure reduction of viscosity of epoxy in order to allow particles for good dispersion and sufficient interaction with the resin. Then the desired mass fraction of TWN flour was added with loadings of 10, 20 and 30 wt% along with small amount of solvent. The mixture was vigorously stirred using mechanical stirrer for 30 min at 80°C temperature. After that, ultrasonication of mixture was done for 30 min at 60°C temperature. Finally stoichiometric amount of hardener DDM was added in the mixture using Eq. (1) and stirred for additional 20 min at 80°C temperature to make it completely soluble. After going through these steps, the mixture was kept in the vacuum oven at 70°C for 10 min to remove entrapped gases to ensure the void free composites.

$$\text{Parts by weight of hardner for 100 parts of epoxy} = \frac{\frac{\text{Molecular weight of Hardener}}{\text{Number of available hydrogens per molecule}}}{\text{Epoxy equivalent weight}} * 100 \quad (1)$$

Solution casting was done to cure the samples. The sequence of curing which we followed was 80°C for 2 h, 110°C for 1 h and 130°C for 4 h. We followed this procedure because filler need some time in step up of heating rate otherwise it may induce some degradation effects during curing. The procedure is slightly different than the conventional procedure for this resin/hardener combination described in the literature [28]. For comparison, neat sample of Ep and DDM was also made using this procedure.

For preparation of composites of P-ddm and Ep mixtures, the monomer containing Ep/P-ddm was degassed in a vacuum oven at 90°C for 6 h. The desired mass fractions of TWN i.e. 10, 20 and 30 wt% along with small amount of solvent was poured into preheated mold at 80°C and cured by heating isothermally at 160°C for 2 h, then pressed at 12 MPa, and heated at 175 and 200°C for 2 h at each stage [29]. The composites were removed from the mold and coded as Ep/P-ddm/TWNX, where X denotes the wt% of TWN.

2.3 Characterization of WN, TWN and composites

In order to compare the chemical structure of walnut shell before and after treatment with alkali and the composites made from it, Fourier transform infrared (FTIR) spectrum analysis was applied by casting a thin film of WN, TWN and all the composites. Powder of each item was mixed with KBr and the prepared film was examined on Perkin-Elmer Spectrum 100 spectrometer (Waltham, MA, USA). The spectra were recorded at 4 cm^{-1} resolution in the range of 4000–450 cm^{-1}.

XRD analysis was applied using X'Pert High Score PW3209 diffractomter to assess WN and TWN crystallinity. The equatorial diffraction patterns (2θ) were recorded from 10 to 40° using Cu-Kα radiation at 40 KV and 20 mA. The Crystallinity indices (*CI*) were calculated according to the Segal empirical method:

$$CI\ \% = 100[\frac{I_{002} - I_{am}}{I_{002}}] \quad (2)$$

where I_{002} is the maximum intensity of the 002 lattice reflection of the cellulose crystallographic form (I_{002}) at 2θ=22° and I_{am} is the intensity of diffraction of the amorphous at 2θ=18°.

Differential scanning calorimetry (DSC) measurements were performed on differential scanning calorimeter model TA Q200, TA Instruments, USA, under 50 mL/min steady flow rate of nitrogen. The sample was carefully weighed (~5 mg) into a sample pan at a room temperature and was tested immediately. The specimens were tested from 30 to 300°C at 20°C/min heating rate.

Thermogravimetric analysis (TGA) was performed on TA Instruments Q50 at a heating rate of 20°C/min from 40 to 800°C under a constant nitrogen flow rate of 50 mL/min. The thermomechanical properties of the samples were analyzed under bending mode by dynamic mechanical analyzer (DMA) model Q800 from TA Instruments, USA. The polished rectangular specimen in the dimension $30 \times 10 \times 2$ mm^3 were loaded in a single cantilever mode, at heating rate of 3°C/min in the range of 40– 200 or 240°C, as required; under nitrogen atmosphere, The strain was applied sinusoidal with a frequency of 1 Hz in air.

3. Results and discussions

3.1 Physical and chemical characterization of WN & TWN flour

The thermogravimetric analysis was done to check the thermal stability of the WN and TWN and the results are shown in Fig. 1 and Table 1. The TGA graph shows 2 steps of degradation for WN while single step was seen for TWN which accounts for treatment of NaOH and resulting rougher surface with reduced water uptake of particles. The values of $T_{5\%}$ and $T_{10\%}$ of TWN increases from approx: 72°C and 227°C to 259°C and 281°C. Furthermore in Fig. 1 (B) DTG, the degradation of WN starts around 126°C and reaches to maximum value at 326°C and finally degrades to maximum temperature of 378°C. For TWN, the initial degradation starts at 173°C which is around 47 degrees higher than the WN, which accounts for better stability of the treated particles. The maximum degradation temperature of TWN was recorded as 320°C while final degradation temperature was recorded as 373°C. As reported in the literature, NaOH treatment removes sufficient amount of lignin from lignocellulosic material. This accounts for shift of maximum and final degradation temperature values to lower temperature. But overall, the initial $T_{5\%}$ and $T_{10\%}$ is improved along with good roughness of the TWN which may account for better reinforcement effects with resins [30].

The changes in the structure of WN and TWN treatment were studied through FTIR and depicted in Fig. 2. The broad transmission band located in the region from 3000-3600 cm^{-1} and around 1043 cm^{-1} indicates bonded -OH groups existing in the WN and TWN flour [31]. No change is detected in the intensity of this band after the treatment. The characteristic peak located at 1730 cm^{-1} is assigned to carbonyl C=O groups in the organic filler which disappears after alkali treatment and confirms hemicellulose removal from the material [31]. Moreover symmetric stretch of =C-O-C groups corresponding to ester, ether and phenol groups in WN are observed at 1250 cm^{-1} which decreases in intensity for TWN. The peak at 1244 cm^{-1} is assigned to acetyl groups of lignin which decreases in intensity showing clearly that lignin was decreased after alkali treatment [26]. The band at 895 cm^{-1} represents glycosidic $–C_1–H$ deformation and –OH bending. These features are the characteristics of β-glycosidic linkages between the anhydroglucose units in cellulose and their intensity peak increases after treatment showing surface activation of cellulose units [32]. Moreover, removal of hemicellulose by alkali treatment results in increased hydrogen bonds between cellulose chains [33]. These observations confirmed that the structure of TWN was altered with more functional groups on the surface for good interactions.

The results of XRD analysis are given in Fig. 3. The *CI* % values are calculated using Eq. (2) and presented in Table 1. It can be seen in Fig. 3, WN exhibit a typical cellulose I pattern, well defined peaks at 2θ=22°. The reflections peak at 22° corresponds to the 002 crystallographic plane of the cellulose I lattice. Increased value of the intensity is clearly observed for TWN treated with 1% NaOH. The *CI* % calculated by Eq. (2) for the TWN, increased about 9%. This increase in *CI* % indicates improvement in the crystalline structure of cellulose and ultimately contributes in performance enhancement of the composites.

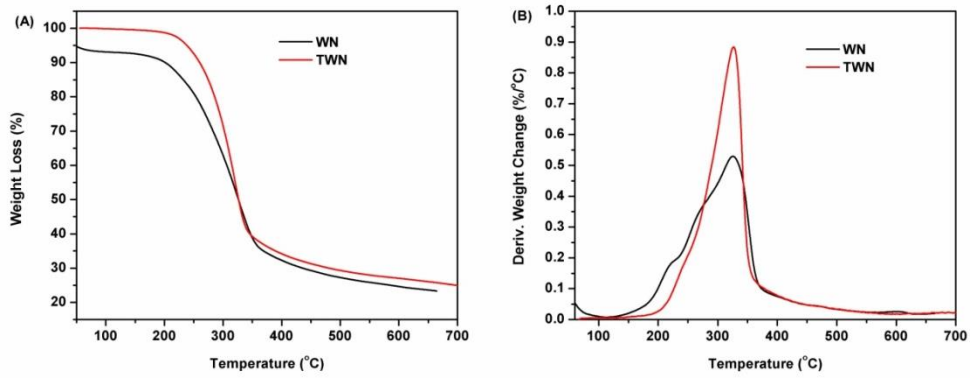

Fig. 1. TGA (A) and DTG (B) of walnut shell before and after alkali treatment

Table 1. TGA, DTG and CI % of walnut flour particles before and after alkali treatment

Sample	$T_{5\%}$ (°C)	$T_{10\%}$ (°C)	Y_c (%) at 600°C	**Cellulose DTG peak** (°C)	***CI* %**
Untreated (WN)	72	227	25.0	326	58
Alkali Treated (TWN)	259	281	26.9	320	67

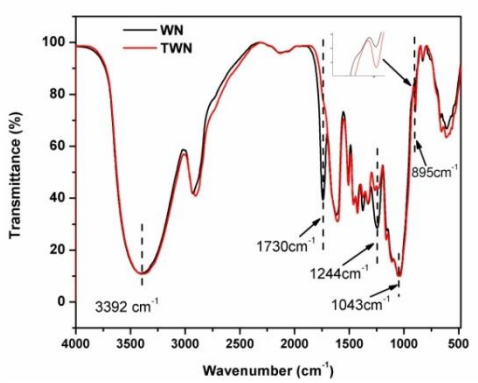

Fig. 2. FTIR of walnut shell before and after alkali treatment

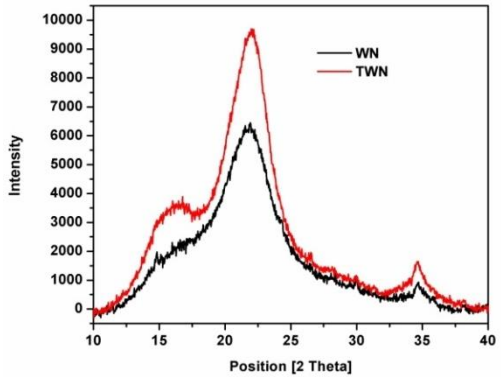

Fig. 3. XRD of walnut shell before and after alkali treatment.

3.2 Differential scanning calorimetry

The DSC was implemented to evaluate the curing behavior of Epoxy and blends with different weight ratios of TWN. The DSC curves and data for Ep/DDM/TWN series blends are presented in Fig. 4 and Table 2, respectively.

All Ep/TWN blends produced lower exothermic peaks and onset temperatures in confront to neat monomer. The onset temperatures and exothermic peaks were decreased by increasing the amount of TWN from 0 to 30 wt% and recorded as 110 and 188°C to 93 and 177°C, respectively. This drop in the initial exotherms and peak temperatures for composites blends is the result of catalytic effect of -OH group of TWN flour, which may accelerate the polymerization process of epoxide rings. It was also observed that increase in TWN loading decreases the heat of polymerization (ΔH) and height of the exothermic peaks due to the polymerization process of composites blends. The highest value of the exothermic peak was observed at 189.06°C for neat Ep/DDM, while the lowest value was recorded at 177.8°C for TWN 30 wt% loading while the ΔH was recorded in the range from 535.6 to 407.7 J/g for Ep/DDM and 30 wt% TWN content composite, respectively. This type of result is never reported before for TWN flour which accelerates the curing process of epoxide monomer in the presence of DDM hardener. Similar catalytic effect of –OH groups of cellulose and lignin on cure reaction of thermosets was also demonstrated in the literature [23, 34]. These observations were also confirmed from the conversion graphs plotted in Fig. 4 (B) where the addition of TWN shifts the conversion/polymerization to lower temperatures except for 30 wt% which after approx 60% conversion shifts to higher temperature may be subjected to increase of viscosity which suppresses the conversion at a given temperature compromising the promoting effects of –OH groups and retards the curing process but still it is far less than the neat resin [35].

Furthermore, DSC results of Ep/P-ddm containing stoichiometric amount of DDM are also evaluated to see the desired effects of blends. The results are summarized in Fig. 5 and 6 and Table 3, respectively. Initially the effects of P-ddm addition in Ep were analyzed and then the selected blend based on lowest reaction enthalpy was selected and analyzed for reinforcement with 10, 20 and 30 wt% TWN. As expected, the system containing stoichiometric amount of DDM in mixture, two peaks are visible in the system Fig 5. Interestingly, the shape of the copolymer varies with the composition of blend. For the system containing P-ddm in lower amount just 10%, only single exothermic peak having a peak temperature (T_p) value of 179°C was observed which is less than the T_p value of Ep/DDM 189°C shown in Fig. 4. Whereas two highly exothermic peaks can be observed when the content of P-ddm increases in the system and both the peaks shifts to slightly higher temperature. In this concern, the copolymerization reaction of Ep/P-ddm proceeds by not only the ring opening reaction of oxaxine ring of P-ddm but etherification reaction of oxirane of Ep and phenolic hydroxyl groups formed by oxazine ring opening reaction. Thus in the system, the first exothermic peak corresponds to ring opening reaction of oxirane of Ep while the second exothermic peak corresponds to oxazine ring opening reaction and radical polymerization of P-ddm.

Table 2. DSC parameters of EP/DDM and TWN blends at different weight content

Sample Code	T_i (°C)	T_p (°C)	ΔH (J/g)
Ep/DDM	110	189.0	535.6
Ep/TWN 10	99	184.6	493.9
Ep/TWN 20	93	180.4	435.1
Ep/TWN 30	93	177.8	407.7

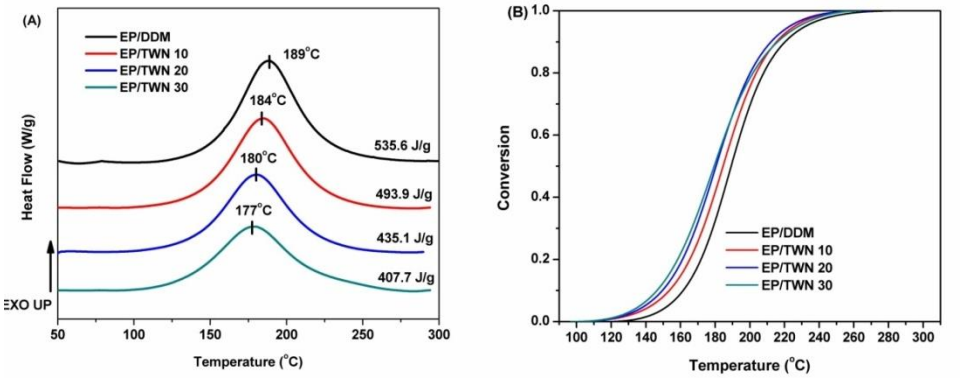

Fig. 4. DSC and conversion of Ep/DDM and TWN blends at different wt%

The characteristics shift of peaks to slightly higher temperature depends on the composition of blend, as the reaction between Ep and P-ddm is catalyzed by lowering the reaction enthalpy of the system by the formation of phenolic hydroxyl groups. For Ep/P-ddm blend with lower P-ddm fraction such as 10%, it is expected that all the P-ddm was consumed in the formation of phenolic hydroxyl groups by ring opening reaction of oxazine ring proceeding quickly and the peak associated with it cannot be discerned in DSC curve. For the blends containing 20 and 30 wt% P-ddm, a relative decrease in first exothermic peak temperature shows the catalytic activity of the formed compounds by the action of P-ddm in blends while this effect can be devoted to decrease in ΔH of the blends. This trend of decrease in ΔH was continued on 40 and 50 wt% of P-ddm blends confirming the catalytic activity of phenolic hydroxyl groups formation in the blends by P-ddm. This result is partially supported by the reaction scheme as shown in Scheme I.

In addition, ΔH of the Ep/P-ddm blends with composition of 90/10, 80/20, 70/30, 60/40 and 50/50 are 565, 552, 543, 532, and 495 J/g, respectively. The ΔH values are constantly decreasing as the amount of P-ddm increases in the system. The system containing 40 and 50 wt% P-ddm shows the values even decreased than the Ep/DDM value of 535 J/g. Based on the reactions involved in the system, the ΔH of the copolymers is the enthalpy change occurring due to oxazine ring opening reaction and the formation of phenolic hydroxyl groups formation which catalyzes the ring opening reaction of oxirane rings of Ep. As many reactions are involved in the copolymerization of formed blends than in the polymerization of Ep and DDM, the structure of the blends Ep/P-ddm is more complex than Ep/DDM. While the ΔH of the system containing 50 wt% P-ddm is minimum than all the systems therefore this was selected to check the desired effects of TWN flour in Ep/P-ddm blends.

The effects of TWN flour on 50/50 Ep/P-ddm blends were studied and the results are summarized in Fig. 6 and Table 3, respectively. As can be seen, all the systems containing TWN flour in blends lowers the ΔH ranging from 384 J/g for the addition of 10 wt% TWN to 319 J/g for 30 wt% TWN addition in confront to 495 J/g with no TWN in the blend in Fig. 5. In addition to this the exothermic peaks corresponding to Ep:DDM is shifted to lower temperatures while for P-ddm slightly moves to higher temperature confirming the reaction of -OH groups of TWN flour which have more reactivity towards Ep/DDM than to P-ddm in the blends while the reaction enthalpies of the blends are lowered. In conclusion it can be stated that the hydroxyl groups of cellulose of TWN flour actively catalyzes the cure reaction of Ep/P-ddm blends by forming some complex compounds in the system.

Table 3. DSC parameters of Ep/P-ddm at different P-ddm content and Ep/P-ddm 50:50 at different TWN content

Sample Code	T_i (°C)	T_{p1} (°C)	T_{p2} (°C)	ΔH (J/g)
Ep/P-ddm 90:10	88	179	-	565
Ep/P-ddm 80:20	86	176	233	552
Ep/P-ddm 70:30	81	176	233	543
Ep/P-ddm 60:40	75	177	237	532
Ep/P-ddm 50:50	72	180	238	495
Ep/P-ddm / TWN 10	75	181	237	384
Ep/P-ddm / TWN 20	103	177	240	365
Ep/P-ddm / TWN 30	105	176	239	319

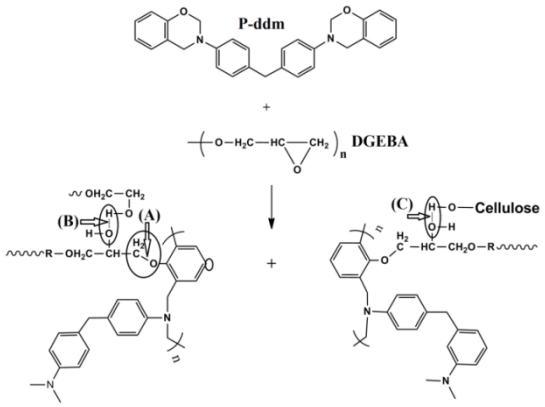

Scheme I. Schematic diagram illustrating the possible process of copolymerization. etherification hydroxyl-oxazine reaction (A), self-associated hydroxyl groups of epoxy (B), Intermolecular hrdrogen bonds with cellulose (C)

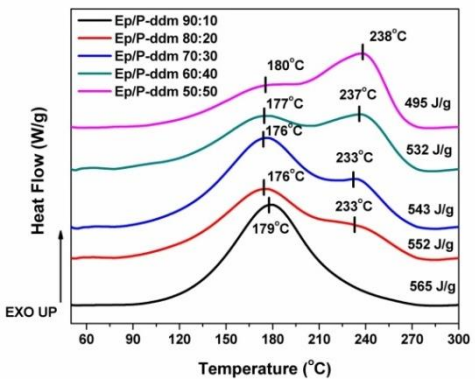

Fig. 5. DSC exotherms of Ep/P-ddm at different wt% content of P-ddm

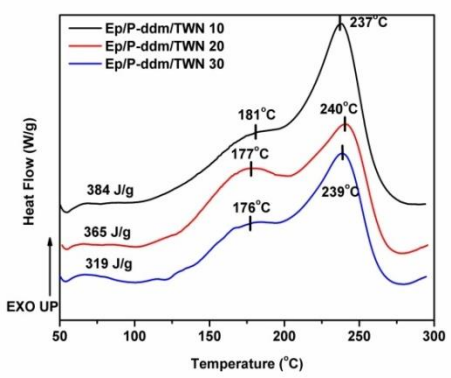

Fig. 6. DSC exotherms of Ep/P-ddm 50:50 at different wt% content of TWN

3.2 Fourier Transform Infrared Spectroscopy

The FTIR studies were also conducted to detect the changes and effects of TWN flour on Ep/DDM and Ep/P-ddm composites. The effect of TWN on Ep/DDM composite is depicted in Fig. 7. C-O stretching vibration of oxirane group of epoxy is clearly visible at 915 cm^{-1} in monomer (a) while it is absent in the cured composites of pure Ep/DDM (b) and Ep/TWN (c) containing epoxy network along with increase in intensity of absorption at 3391 cm^{-1} which confirms the curing of Ep/DDM and Ep/TWN composites along with formation of –OH group during the cure reaction [36, 37]. Stretching vibrations of -OH is located in the region of 3550 to 3409 cm^{-1}. Saturated C-H stretching vibrations are located in the region of 2979-2864 cm^{-1} while unsaturated =C-H stretching vibrations are located at 3030 cm^{-1}. C-O-C stretching vibrations of ethers are located at 1036 cm^{-1} while characteristics peak at 1609 and 1509 cm^{-1} correspond to C=C and C-C of aromatic rings. The characteristic shift of -OH vibrations at 3409 of Ep/DDM cured network without TWN (b) to lower wave number 3349 cm^{-1} in TWN containing network (c) clearly indicates the increase of hydrogen bonding between TWN and Ep/DDM composites [38, 39]. This shows that intermolecular and/or intramolecular hydrogen bonding occurs between cellulose and lignin of TWN flour and Ep/DDM network [23, 40].

The structural changes of pure P-ddm, Ep/P-ddm and Ep/P-ddm/TWN cured structures can be perceived from the variation of intensities of characteristics absorption peaks in FTIR spectra as shown in Fig. 8. The region between 4000-2500 cm^{-1} assigned to –OH stretching vibrations resulted in generation of hydroxyl groups by oxirane ring opening reaction as the reactions proceeds. Incorporation of P-ddm in Ep generates this region while the characteristic shift of this peak from 3426 cm^{-1} in Ep/P-ddm network to 3372 cm^{-1} in Ep/P-ddm/TWN cured network represents intermolecular and/or intramolecular hydrogen bonding [39, 41]. Furthermore, the characteristic absorption band at 950 cm^{-1} corresponds to benzene ring to which oxazine ring is attached and 1228 cm^{-1} assigned to asymmetric stretching of the ether linkage (C–O–C) also show changes due to presence of Ep and TWN in the respective cured structures [20, 42, 43]. In addition, ether linkages are observed due to occurrence of peak centered at 1106 cm^{-1} which is more pronounced in TWN containing network as compared to Ep/P-ddm blend. Furthermore CH_2 bending mode of methylene (CH_2) present at 1497 cm^{-1} in P-ddm shifts to 1479 cm^{-1} in Ep/P-ddm while shift to 1471 cm^{-1} in Ep/P-ddm/TWN network which is showing an increase of higher degree of polymerization in TWN containing network as the reaction proceeds by forming methylene bridges in the Ep/P-ddm/TWN network [44, 45] . Formation of small peak in the region 1725 cm^{-1} to 1645 cm^{-1} corresponds to N-H bending vibration which is also more pronounced in TWN containing network then Ep/P-ddm and pure P-ddm composites which also show that TWN have changed the structure of composite blend by forming some complex structures within the system.

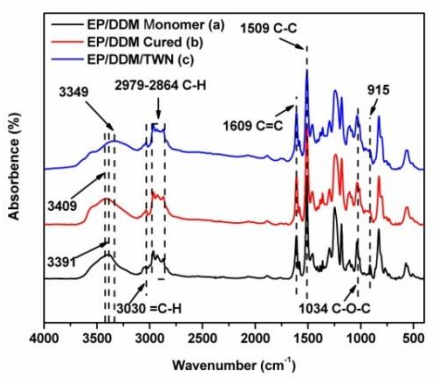

Fig. 7. FTIR of Ep:DDM monomer (a), cured without TWN (b), cured with TWN (c)

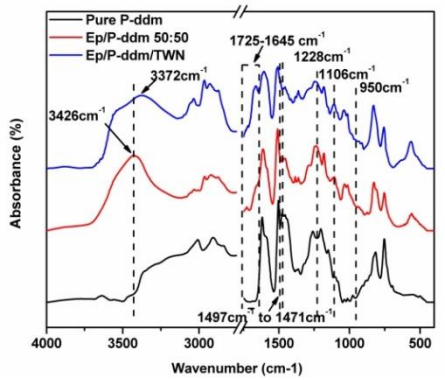

Fig. 8. FTIR of P-ddm, Ep/P-ddm 50:50 and Ep/P-ddm/TWN

3.3 Thermogravimetric analysis

For the formation of high performance thermoset composites, the thermal stability of the fillers is an important function. High performance thermosets often have curing temperatures around 150–220°C, while natural biomasses relatively have higher degradation rate at this range of temperature which restrict their use as an efficient reinforcement in composites [46, 47]. To overcome this problem, fillers must be well treated to remove the constituents having higher degradation rate between 150-220°C. As discussed in section the preparation of TWN, alkali treatment sufficiently improves its stability at this temperature range which ensures minimum degradation of the fillers during processing.

As expected, the formed composites by incorporating TWN were homogenous and bonds breakage in the structure was concurrent representing that TWN have formed cross-links within the network. The TGA curves under nitrogen atmosphere from 50 to 800°C for Ep/DDM and its blends with different wt% of TWN are depicted in Fig. 9 (A) and $T_{5\%}$, $T_{10\%}$, $T_{20\%}$ and Y_c values are summarized in Table 4. As can be seen from Fig. 9 (A) that incorporation i.e. 10 wt% TWN in the network decreases the $T_{5\%}$, $T_{10\%}$ and $T_{20\%}$ while Y_c shows the maximum value 18.47% which is around 85% more than the neat resin. This is because the $T_{5\%}$ and $T_{10\%}$ of the filler particles as depicted in Table 1 is low; 259 and 281°C as compared to pure Ep/DDM, even though it only shows a decrease of 33 and 19°C in $T_{5\%}$ and $T_{10\%}$ temperature weight loss. It is interesting to note that as the filler quantity increases, $T_{5\%}$, $T_{10\%}$ and $T_{20\%}$ shifts to higher temperatures showing improved thermal stability of composites. The $T_{10\%}$ and $T_{20\%}$ of 30 wt% TWN composites show 1 and 8°C increase in the values than composite of Ep/DDM. The possible explanation for this is the constituents of TWN contain mainly cellulose as a major portion and lignin as a minor component. The structure of lignin is aromatic and has many polar bonds (hydroxyl) which interacts with the cross-linked epoxy thereby increasing the aromaticity in the network [48]. However, it is also reported that lignin act as a thermal stabilizer of cellulose against thermal oxidation [49].

Fig. 9 (B) shows DTG curves of Ep/DDM and its blends with different wt% loading of TWN. All the samples show thermal degradation process had only one stage of decomposition as like the Ep/DDM composite. The maximum rate of decomposition value of Ep/DDM (403.15°C) is in good agreement with the value reported in the literature [50, 51]. The decomposition step of all composites was in the range of 250-650°C with maximum degradation rate at 390.0, 400.3 and 404.5°C for 10, 20 and 30 wt% TWN, respectively. The introduction of TWN in the system shifts maximum rate of decomposition slightly toward lower temperature but the rate of decomposition decreases around 24% and 6% for TWN 10 and 20 wt% respectively showing improved thermal stability. Moreover the decomposition rate of all composites are ranging from 250°C to maximum point also shifts to higher temperatures when increasing TWN in the network which is interesting to note as lignocellulosic biomaterial used for reinforcement mostly decreases the thermal stability of composites [23, 52]. Effect of cellulose lowers, while lignin improves the thermal stability. However, TWN contains both as the major constituents which have favorable effects on thermal stability of composites filled with it. The formed composites with TWN, effectively satisfies the requirement of solder-dip resistance and heat resistance properties of electronic material field [52, 53].

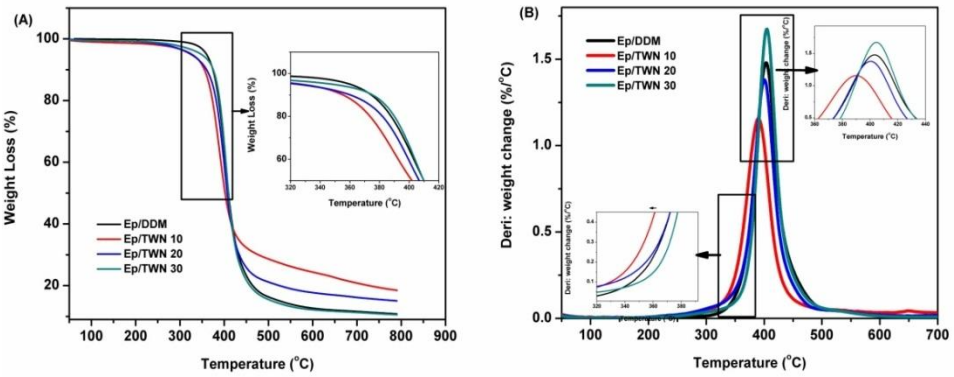

Fig. 9. TGA (A) and DTG (B) of Ep:DDM/TWN at different wt% of TWN

Table 4. TGA summary for Ep/DDM and blends at different wt % of TWN

Sample Code	$T_{5\%}$ (°C)	$T_{10\%}$ (°C)	$T_{20\%}$ (°C)	Y_c (%)	DTG peak (°C)
Ep/DDM	360.2	374.5	387.8	10.85	403.1
Ep/TWN 10	327.2	355.4	373.6	18.47	390.0
Ep/TWN 20	325.0	360.3	382.0	15.06	400.3
Ep/TWN 30	348.3	375.4	390.0	10.55	404.5

The effects of TWN on blends containing 50:50 Ep/P-ddm and the respective composites containing 10, 20 and 30 wt% TWN on thermal stability is shown in Fig. 10 (A) and values of $T_{5\%}$, $T_{10\%}$ and Y_c % are summarized in Table 5. The incorporation of TWN in blends initially i.e. 10 wt% decreases the $T_{5\%}$ and $T_{10\%}$ to minimum and the values reach 329°C and 356°C respectively. Further increase of TWN in composites shifts the values of $T_{5\%}$ and $T_{10\%}$ shifts to higher temperatures. The maximum value recorded for 30 wt% TWN composites were 333°C and 359°C. The effect of TWN in blends is also same as reported earlier for Ep/DDM composites. However, interestingly the char yield of 10 wt% TWN composites, maximum value was recorded i.e. 37.89% which is 47% higher than the value for pure 50:50 blend. This value does not change for 20 wt% TWN blend but decreases for 30 wt% TWN blend. The reason could be the surface particles of TWN 30 wt% in composites have been exposed to higher temperature of cure for longer period which have caused some degradation of surface particles. The increase char yield of 10 and 20 wt% TWN composites is important especially for designing fire retardant composites.

In connection to this, limiting oxygen index (*LOI*) values of composites were calculated and summarized in Table 5. *LOI* is the minimum amount of oxygen required to continue the combustion of materials. It is a parameter to determine the effectiveness of fire retardants and to measure the flammability of the polymeric materials [54]. *LOI* can be calculated by the values of Y_c by applying Van Krevelen and Hoftyzer method [55, 56] Eq. (3) Materials with *LOI* below 20.95% can easily burn in air while the materials having *LOI* above 28% are self extinguishing materials [54].

$$LOI = 17.5 + 0.4Yc \tag{3}$$

From the calculated values of *LOI* it can be seen that all the composites containing TWN falls in the category of self extinguishing materials having values 32.65, 31.62 and 28.37 for TWN 10, 20 and 30 wt% which is an added advantage of TWN in these high performance blends.

A similar effect of TWN in blends was observed in DTG graphs as shown in Fig. 10 (B). The maximum rate of degradation shifts to lower temperature initially for 10 wt% of TWN in blends than it continues to shifts to higher temperature when the content of TWN increases, in fact the maximum amount of TWN, i.e. 30 wt% have same maximum degradation rate as of pure Ep/P-ddm 50:50 blend which is a new finding corresponding to TWN bio organic material. Overall it can be seen that rate of degradation of all the blends is less than the pure Ep/P-ddm blend which is the real reason for increased *LOI* values of all composites as discussed before.

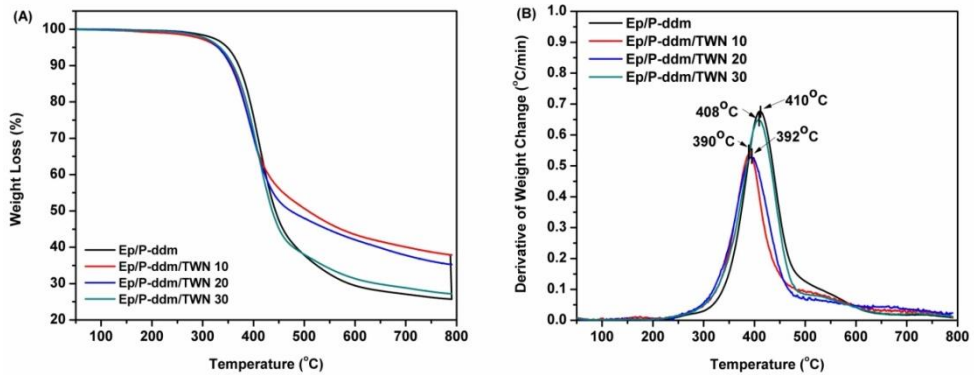

Fig. 10. TGA (A) and DTG (B) of Ep/P-ddm/TWN at different wt% of TWN

Table 5. TGA summary for Ep/P-ddm and blends at different wt % of TWN

Sample	$T_{5\%}$ **(°C)**	$T_{10\%}$ **(°C)**	$T_{20\%}$ **(°C)**	Y_c **(%)**	**DTG Peak (°C)**	***LOI* (%)**
Ep/P-ddm 50:50	348	371	391	25.7	410	27.72
Ep/P-ddm/TWN 10	329	356	379	37.8	390	32.65
Ep/P-ddm/TWN 20	330	355	379	35.3	392	31.62
Ep/P-ddm/TWN 30	333	359	384	27.1	408	28.37

3.4 Dynamic mechanical analysis

Fig. 11 (A) and (B) shows storage modulus (G') and loss factor ($tan\ \delta$) curves as a function of temperature (T) of Ep:DDM and Ep/TWN. All the composites along with pure Ep/DDM, the G' values decrease slowly in the glassy state, and then decrease rapidly at different temperatures for various compositions. Poor compatibility between TWN and Ep/DDM was shown in the rubbery plateau region while storage modulus continues to rise in glassy state by incorporating TWN in the composites. The value reaches up to 2213 MPa from 1532 MPa for 20 wt% of TWN which was 44.45% more than the pure Ep/DDM composite. Increased storage modulus in glassy state is related to increased crosslinking density of the system. For this Nielsen and Landel describe the

approximate relationship [57] Eq. (4), which is reported to better describe the elastic properties of dense networks [58]

$$\log\frac{G}{3} = 7.0 + 293(\rho) \tag{4}$$

where G' is storage modulus (dynes cm^{-2}) and ρ is the crosslinking density (mol cm^{-3}). The values are summarized in Table 6. All the composites with TWN show increased crosslinking density confirming the stiffness increase of the composites.

Table 6. DMA parameters for Ep/DDM and its blends with TWN at different wt%

Sample	G' (GPa) [a]	The gain in G' (%)	T_g (°C) [b]	ρ ($\times 10^{-3}$ mol/cm^3)
Ep/DDM	1.53	-	147	4.70
Ep/TWN 10	1.78	16.33	147	5.43
Ep/TWN 20	2.21	44.44	146	5.86
Ep/TWN 30	2.18	42.48	146	-

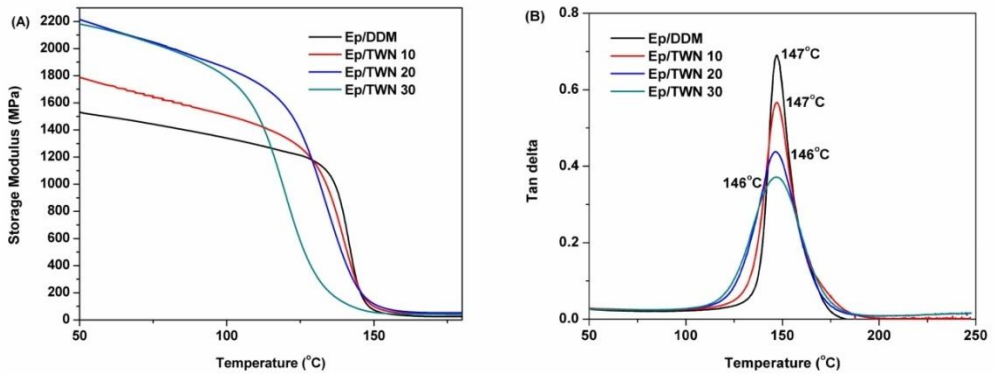

Fig. 11. Storage Modulus (A) and Tan Delta (B) of Ep/DDM and Ep/TWN at different wt% of TWN

Moreover, a single dissipation energy peak is shown on each *tan δ* curve Figure 11 (B), associated with the glass transition for TWN composites, indicating no detectable particle separations for these composites. T_g is defined as the temperature corresponding to the maximum of *tan δ* peak. The T_g of TWN composites did not show any decrease while the peak height was reduced and broadened, reflecting increased number of modes of branching and wider distribution of structures between TWN and Ep/DDM. However, decreased T_g of the system does not reflect low storage modulus of the system which means that the surface of the filler was functionalized to a greater extent by alkali treatment except the core of the particles which influences overall cross linking points within the system [59, 60]. Another suitable explanation of this behavior is as the mold was preheated at 80°C which is the polymerization temperature of DDM. At this temperature the viscosity of Ep was low, which allowed fast reaction of DDM to Ep than the TWN to Ep so the system does not acquire increased T_g. Additionally, the overall interaction of TWN with epoxy show weak interface because of the formation of –OH interactions with Ep/DDM network where no covalent bond formation was detected [61]. This finding is also important in continuous process of composites for commercial applications where the T_g of these composites does not fall even

when absolutely no time was given for relaxation/gelation and process was continuous. Further work in this area is needed to find out the effect of gelation time on these materials which would be helpful to understand the behavior of TWN for improved T_g of the composites.

The blends of Ep/Pddm and composites containing TWN were also investigated by DMA to study the variation in the storage modulus (G') and loss factor ($tan\ \delta$), as shown in Fig. 12 (A) and (B) while the values are summarized in Table 7. As shown in Fig. 12 (A) and (B), the TWN reinforcement in blends significantly improved the G' and T_g. Likewise, G' of pure Ep/P-ddm and its blends with TWN reduces as a function of increased temperature, this could be connected to the softening of matrix. The pure Ep/P-ddm showed 2.08 GPa and 171°C as stiffness at 50°C and T_g, respectively. Interestingly all the composites with TWN showed higher G' values than the pure Ep/P-ddm blend indicating that combination of TWN to Ep/P-ddm leads to better stress transfer may be due to hydrogen bonding and methylene linkages as discussed previously in FTIR section [23]. The values of crosslinking densities of the respective composites are summarized in Table 7.

Loss factor ($tan\ \delta$) peak values for all composites with TWN shows the T_g of the composites shifts to higher temperatures as compared to Ep/P-ddm composite. The shifting of $tan\ \delta$ can be related to good surface interactions of TWN. Moreover, the heights of all the composites were decreased compared to Ep/P-ddm blend which shows increased interaction along with stiffness improvement. Peak height of 30 wt% blend was reduced to 0.49 from 0.85. Furthermore, composites with 30 wt% TWN show T_g value of 201°C compared to blend with no TWN (171°C). The behavior of TWN in blends of Ep/P-ddm restricts the chain mobility of the system which is the result of good particles interactions [62]. However dilution phenomena of TWN in Ep/P-ddm is more prominent compared to Ep/DDM blends discussed previously which also results in the broadening of $tan\ \delta$ peak [63]. This type of behavior of TWN may have been resulted for blends of Ep/P-ddm than with Ep/DDM as more time was given in the curing stage along with step up of temperatures so the interactions of TWN with resin blends was prominent. Furthermore, the polymerization temperature of blend was far enough which must have allowed TWN to form cross-links in three dimensions and improved the T_g.

In connection to this thermal deformation temperature (T_d) of the formed composites was measured to evaluate the heat resistance of all the composites and the values are summarized in Table 8. The definition of T_d is the temperature of a standard sample bending to a level at a certain physical strength [64]. According to ASTM 648, T_d is the temperature of a material at 0.933 GPa storage modulus. T_d can be acquired from the DMA curves of materials. Although all the composites showed different value of initial modulus, the composites of Ep/DDM containing 20 wt% TWN, T_d value just drops 2 degrees from the parent composite. While for blends of Ep/P-ddm, T_d shows an obvious gap of 23°C increase for composite containing 30 wt% of TWN. These values also confirmed the positive effect of the TWN to the thermal property of composites.

Table 7. DMA parameters for Ep/P-ddm and its blends with TWN at different wt%

Sample	**G' (GPa) [a]**	**The gain in G' (%)**	**T_g (°C) [b]**	**ρ ($\times 10^{-3}$ mol/cm^3)**
Ep/P-ddm	2.08	-	171	5.68
Ep/P-ddm /TWN 10	2.47	18.75	191	6.47
Ep/P-ddm /TWN 20	2.67	28.36	193	6.08
Ep/P-ddm /TWN 30	3.30	58.65	201	5.94

Table 8. Thermal deformation temperatures (T_d) of the composites

Sample Name	T_d (°C)
Ep/DDM	137.7
Ep/TWN 10	135.1
Ep/TWN 20	132.7
Ep/TWN 30	119.9
Ep/P-ddm	159.5
Ep/P-ddm /TWN 10	170.2
Ep/P-ddm /TWN 20	173.2
Ep/P-ddm /TWN 30	182.2

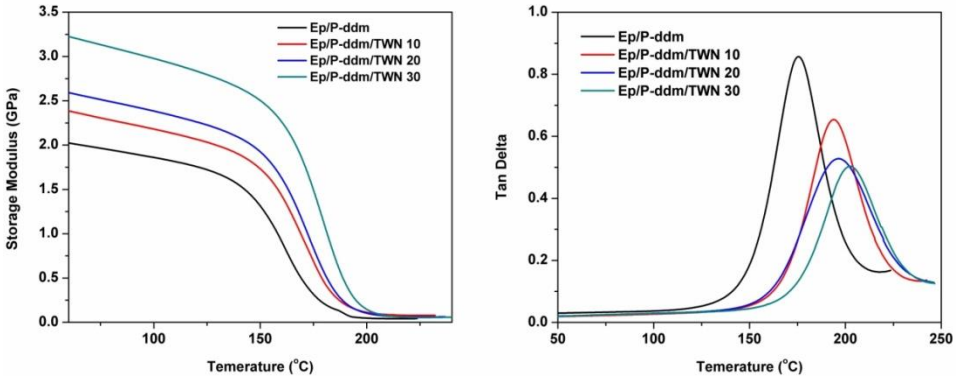

Fig. 12. Storage Modulus (A) and Tan Delta (B) of Ep/P-ddm and Ep/P-ddm/TWN at different wt% of TWN

4. Conclusions

High performance thermosets based on Ep/DDM and Ep/P-ddm 50:50 system were successfully reinforced with TWN particles from 10 to 30 wt%. Alkali treatment of TWN confirms the removal of hemicelluloses and a part of lignin from the shell particles. TWN improves in thermal stability as studied by TGA after 1% alkali treatment. The alkali treatment of WN also increases the crystallinity index *CI* % of the particles to 67% from 58% of untreated WN. Studies of DSC show the reinforcement of TWN in both of the high performance system catalyses the curing procedure by decreasing the reaction enthalpies of the systems. FTIR studies of shell particles before and after alkali treatment were compared for structural changes which show increased functionalization of shell particles after the alkali treatment. FTIR studies also confirmed the increased hydrogen bonding of TWN with Ep/DDM system. Increased hydrogen bonding along with sufficient methylene linkages were observed in Ep/P-ddm composites containing TWN.

Thermal stability studies by TGA reveal that incorporation of TWN in these high performance systems shift the maximum degradation rate to higher temperatures which design a new bio based composites system fit for solder drip resistance and fire retardant applications. Decrease of 20 to 30 wt% for the system of Ep/DDM, the storage modulus G' of composites gain 44 to 42% increase while T_g value of system remain unaffected while similar behavior was also observed for T_d of the composites which is an added advantage when considering thermal properties of the composites. Decrease of 30 wt% for the system of Ep/P-ddm blend with TWN, the storage modulus increases about 58% while T_g value also increases 30°C along with T_d which increases 23°C from the parent composites. In short, novel composite system based on TWN can be designed with improved thermal and thermomechanical behavior with considerable amount of weight savings.

References

[1] S. Chaitanya, I. Singh, Polymer Composites, 1-12 (2017).
[2] H. Khanjanzadeh, T. Tabarsa, A. Shakeri, Journal of Reinforced Plastics Composites **31**, 341 (2012).
[3] H. Pirayesh, A. Khazaeian, Composites Part B: Engineering **43**, 1475 (2012).
[4] J. Adhikari, B. Biswas, S. Chabri, N. R. Bandyopadhyay, S. Halder, B. C. Mitra, A. Sinha, Polymer Composites (2017).
[5] M. Gürü, S. Tekeli, İ. Bilici, Materials & Design **27**, 1148 (2006).
[6] A. Qaiss, R. Bouhfid, H. Essabir, Characterization and Use of Coir, Almond, Apricot, Argan, Shells, and Wood as Reinforcement in the Polymeric Matrix in Order to Valorize These Products, in: "K.R. Hakeem, M. Jawaid, O. Y. Alothman (Eds.), Agricultural Biomass Based Potential Materials, Springer International Publishing, Cham", 305 (2015).
[7] M. A. Berthet, H. Angellier-Coussy, V. Chea, V. Guillard, E. Gastaldi, N. Gontard, Composites Part A: Applied Science and Manufacturing **72**, 139 (2015).
[8] R. M. Gurjar, Bioresource Technology **43**, 177 (1993).
[9] E. Sancak, A. Onat, S. Ersoy, A. Beyit, Asian journal of Chemistry **25**, (2013).
[10] M. A. Mosiewicki, N. E. Marcovich, M. I. Aranguren, Journal of Applied Polymer Science **121**, 2626 (2011).
[11] Y. Nie, X. Tian, Y. Liu, K. Wu, J. Wang, Polymer Composites **34**, 77 (2013).
[12] FAOSTAT data,http://www.fao.org/faostat/en/#data/QC/ Accessed on 04/27/2017.
[13] A. Demirbaş, Energy Sources **27**, 761 (2005).
[14] N. Ayrilmis, A. Kaymakci, F. Ozdemir, Journal of Industrial and Engineering Chemistry **19**, 908 (2013).
[15] M. Gürü, M. Atar, R. Yıldırım, Materials & Design **29**, 284 (2008).
[16] A. J. Mohammed, International Journal of Science and Technology **3**, 18 (2014).
[17] P. C. Gope, V. K. Singh, D. K. Rao, Journal of Reinforced Plastics and Composites **34**, 1075 (2015).
[18] M. Doddamani, G. Parande, V. Manakari, I. G. Siddhalingeshwar, V. N. Gaitonde, N. Gupta, Materials Performance and Characterization **6**, 2017.
[19] S. Tragoonwichian, N. Yanumet, H. Ishida, Composite Interfaces **15**, 321 (2008).
[20] C. H. Lin, S. L. Chang, C. W. Hsieh, H. H. Lee, Polymer **49**, 1220 (2008).
[21] S. B. Shen, H. Ishida, Polym. Compos **17**, 710 (1996).
[22] H. Ishida, S. Rimdusit, Thermochim. Acta **320**, 177 (1998).
[23] A. Q. Dayo, B. C. Gao, J. Wang, W.-B. Liu, M. Derradji, A. H. Shah, A. A. Babar, Composites Science and Technology **144**, 114 (2017).
[24] S. Grishchuk, L. Sorochynska, O. C. Vorster, J. Karger-Kocsis, Journal of Applied Polymer Science **127**, 5082 (2013).
[25] T. Agag, T. Takeichi, Macromolecules **36**, 6010 (2003).
[26] W. Liu, A. K. Mohanty, L. T. Drzal, P. Askel, M. Misra, Journal of Materials Science **39**, 1051 (2004).
[27] A. Jabbar, J. Militký, B. Madhukar Kale, S. Rwawiire, Y. Nawab, V. Baheti, Industrial Crops and Products **84**, 230 (2016).
[28] H. Dong, Y. Li, J. Zhang, L. Liu, L. Cao, P. Ming, W. Liu, C. Zhang, L. Liu, H. Wei, RSC Advances **6**, 65533 (2016).
[29] A. Q. Dayo, Y. L. Xu, A. Zegaoui, A. A. Nizamani, J. Wang, L. Zhang, W.-B. Liu, A. H. Shah, Plastics Rubber and Composites, 1-8 (2017).
[30] Z. N. Azwa, B. F. Yousif, Polymer Degradation and Stability **98**, 2752 (2013).
[31] Y. Seki, M. Sarikanat, K. Sever, C. Durmuşkahya, Composites Part B: Engineering **44**, 517 (2013).
[32] S. Elanthikkal, U. Gopalakrishnapanicker, S. Varghese, J.T. Guthrie, Carbohydrate Polymers **80**, 852 (2010).
[33] J. Gassan , A. K. Bledzki, Journal of Applied Polymer Science **71**, 623 (1999).
[34] F. Ferdosian, Y. Zhang, Z. Yuan, M. Anderson, C. Xu, European Polymer Journal **82**, 153 (2016).

[35] D. Bertomeu, D. García-Sanoguera, O. Fenollar, T. Boronat, R. Balart, Polymer Composites **33**, 683 (2012).
[36] Q. Guo, Polymer **36**, 4753 (1995).
[37] J. Qin, G. Zhang, R. Sun, C. Wong, Journal of Thermal Analysis and Calorimetry **117**, 831 (2014).
[38] J. B. María González, Applications of FTIR on Epoxy Resins – Identification, Monitoring the Curing Process, Phase Separation and Water Uptake, INTECH, Spain, p. 510 (2012).
[39] L. LI, Q. WU, S. LI, P. Wu, Applied Spectroscopy **62**, 1129 (2008).
[40] I. Korbag, S. M. Saleh, International Journal of Environmental Studies **73**, 226 (2016).
[41] T. Holopainen, L. Alvila, J. Rainio, T.T. Pakkanen, Journal of Applied Polymer Science **69**, 2175 (1998).
[42] B. Kiskan, B. Koz, Y. Yagci, Journal of Polymer Science Part A: Polymer Chemistry **47**, 6955 (2009).
[43] X. Wu, Y. Zhou, S. Z. Liu, Y. N. Guo, J.-J. Qiu, C. M. Liu, Polymer **52**, 1004 (2011).
[44] A. Kaushik, P. Singh, G. Verma, Rekha, Journal of Thermoplastic Composite Materials **23**, 79 (2009).
[45] K. S. Santhosh Kumar, C. P. Reghunadhan Nair, K. N. Ninan, Thermochimica Acta **441**, 150 (2006).
[46] M. Tajvidi, R. H. Falk, J. C. Hermanson, Journal of Applied Polymer Science **101**, 4341 (2006).
[47] J. Biagiotti, S. Fiori, L. Torre, M. A. Lopez, J. M. Kenny, Polymer Composites **25**, 26 (2004).
[48] H. Pan, G. Sun, T. Zhao, G. Wang, Polymer Engineering & Science **55**, 924 (2015).
[49] Z. Czégény, E. Jakab, M. Blazsó, Journal of Analytical and Applied Pyrolysis **103**, 52 (2013).
[50] P. Sharma, V. Choudhary, A. K. Narula, Journal of Applied Polymer Science **107**, 1946 (2008).
[51] F. Ferdosian, Z. Yuan, M. Anderson, C. C. Xu, Journal of Analytical and Applied Pyrolysis **119**, 124 (2016).
[52] C. Asada, C. Sasaki, Y. Uto, J. Sakafuji, Y. Nakamura, Biochemical Engineering Journal **60**, 25 (2012).
[53] C. Sasaki, M. Wanaka, H. Takagi, S. Tamura, C. Asada, Y. Nakamura, Industrial Crops and Products **43**, 757 (2013).
[54] M. I. Nelson, H. S. Sidhu, R. O. Weber, G.N. Mercer, Anziam J **43**, 105 (2001).
[55] P. Sharma, V. Choudhary, A. K. Narula, J. Appl. Polym. Sci **107**, 1946 (2008).
[56] M. F. Mustafa, W. D. Cook, T. L. Schiller, H. M. Siddiqi, Thermochim. Acta **575**, 21 (2014).
[57] R. F. Landel, Mechanical Properties of Polymers and Composites, C. Press (Ed.) (1993).
[58] C. Jubslip, B. Ramsiri, S. Rimdusit, Polym Eng Sci **52**, 1640 (2012).
[59] K. Salasinska, M. Barczewski, R. Górny, A. Kloziński, Polymer Bulletin, 2017.
[60] P. Agrawal, A. M. Alves, G. F. Brito, S. N. Cavalcanti, A. P. M. Araújo, T. J. A. Mélo, Polymer Composites, 2016.
[61] C. Jiang, D. Jiang, J. Zhang, S. Lin, X. Shang, S. Ju, Polymer Composites, 2017.
[62] M. Ridzuan, M. S. A. Majid, M. Afendi,Compos Structures.**152**, 850 (2016).
[63] N. Saba, M. Jawaid, O. Y. Alothman, Constr Build Mater **106**, 149 (2016).
[64] M. L. Guo, The Dynamic Thermomechanical Analysis of Polymer and Composite Material, China, 2002.